Published in final edited form as:
J Comp Neurol. 2009 September 20; 516(3): 213–225. doi:10.1002/cne.22097.

Vagal gustatory reflex circuits for intraoral food sorting behavior in the goldfish Cellular organization and neurotransmitters

Takanori Ikenaga[1,3], **Tatsuya Ogura**[1,2], and **Thomas E. Finger**[1,*]

[1]Rocky Mountain Taste & Smell Center, Department of Cell and Developmental Biology, University of Colorado Denver School of Medicine, Aurora, Colorado 80045

[2]Department of Biological Sciences, University of Maryland Baltimore County, Baltimore, Maryland 21250

Abstract

The sense of taste is crucial in an animal's determination as to what is edible and what is not. This gustatory function is especially important in goldfish who utilize a sophisticated oropharyngeal sorting mechanism to separate food from substrate material. The computational aspects of this detection are carried out by the medullary vagal lobe which is a large, laminated structure combining elements of both the gustatory nucleus of the solitary tract and the nucleus ambiguus. The sensory layers of the vagal lobe are coupled to the motor layers via a simple reflex arc. Details of this reflex circuit were investigated with histology and calcium imaging. Biocytin injections into the motor layer labeled vagal reflex interneurons which have radially-directed dendrites ramifying within the layers of primary afferent terminals. Axons of reflex interneurons extend radially inward to terminate onto both vagal motoneurons and small, GABAergic interneurons in the motor layer. Functional imaging shows increases in intracellular Ca^{++} of vagal motoneurons following electrical stimulation in the sensory layer. These responses were suppressed under Ca^{++}-free conditions and by interruption of the axons bridging between the sensory and motor layers. Pharmacological experiments showed that glutamate acting via (±)-α-amino-3-hydroxy-5-ethylisoxazole-4-propioinc acid (AMPA)/kainate and *N*-methyl-D-aspartic acid (NMDA) receptors mediates neurotransmission between reflex interneurons and vagal motoneurons. Thus the vagal gustatory portion of the viscerosensory complex is linked to branchiomotor neurons of the pharynx via a glutamatergic interneuronal system.

Keywords

oro-branchial reflex; gustatory; nucleus solitary tract; cyprinid fish; vagal lobe; glutamate

INTRODUCTION

In all vertebrates, the sense of taste plays a pivotal role in the determination of palatability of potential food items. Morsels that carry appetitive cues, e.g., carbohydrates or amino acids, are ingested; those with aversive cues, e.g. bitter plant alkaloids, are rejected. Taste buds situated in the oropharynx and epiglottis, which are innervated by the vagus nerve, are

*Correspondence to: Thomas E. Finger, Department of Cell and Developmental Biology, University of Colorado at Denver and Health Sciences Center, Mailstop 8108, P.O. Box 6511, Aurora, Colorado 80045, Tel. +1 303 724 3436, Fax +1 303 724 3420, Tom.Finger@UCHSC.edu.
[3]Current address: NIH, Section on Model Synaptic Systems, Laboratory of Molecular Physiology, NIH/NIAAA, Bethesda, MD 20892-9411

implicated in triggering reflexive swallowing or gagging (Atema, 1971; Miller, 2002) including the buccopharyngeal phase of swallowing (Altschuler, 2001).

In rodents, the reflex arc connecting the vagal primary gustatory afferents to the motoneurons of the nucleus ambiguus (nAmb) that innervate the pharynx and larynx, involves an obligatory synapse in the nucleus of the solitary tract (nTS) and an obligatory interneuron of the solitary complex or subjacent reticular formation (Barrett et al., 1994; Bao et al., 1995; Hayakawa et al., 1997, 1998; Cunningham and Sawchenko, 2000; Altschuler, 2001). The neurotransmitter for the primary afferent limb is glutamate acting on ionotropic glutamate receptors including both (±)-α-amino-3-hydroxy-5-ethylisoxazole-4-propioinc acid (AMPA)/kainate and *N*-methyl-D-aspartic acid (NMDA) subtypes (Bradley et al., 1996; Smeraski et al., 1996; Li and Smith, 1997; Lu and Bieger, 1998; Smeraski et al., 1998; 1999). The neurotransmitter for the interneuron bridging from the afferent input to the ambigual motoneurons is less well defined. The neurons of the nAmb possess a variety of receptors including glutamate receptors, GABA receptors and cholinergic receptors (Bieger, 1991; Kessler, 1993; Lu and Bieger, 1998), but the key neurotransmitter of the obligatory interneuorn in this gustatory reflex arc is not clear.

In goldfish and related carp, the vagal components of the nTS are relatively hypertrophied compared to other vertebrates reflecting the specialization of the pharynx, called the palatal organ, which enables complex food-sorting behaviors (Sibbing and Uribe, 1985; Sibbing et al., 1986; Lamb and Finger, 1995). These species scoop up materials from the bottom substrate, including food, sand, mud, and gravel. Material is conveyed to the posterior oral cavity and sorted there. Acceptable food particles are transported caudally toward the chewing organ for swallowing, and in contrast non-food are ejected from the mouth (Sibbing and Uribe, 1985; Sibbing et al., 1986; Lamb and Finger, 1995; Callan and Sanderson, 2003). In the sorting phase, large particles are trapped between the palatal organ, (a muscular structure on the roof of the anterior oropharynx), and gill arches, which form the ventral surface of the caudal oral cavity. The palatal organ of goldfish and related carp is highly developed compared to other teleost species, indicating that functional significance of oropharyngeal food sorting behavior of these fish. Although the tactile sense undoubtedly plays a role in the intraoral sorting behavior, goldfish utilize chemical cues to distinguish palatable from unpalatable objects (Lamb and Finger, 1985). Indeed, the palatal organ and roof of gill arches contain high densities of taste buds (Sibbing et al., 1986).

The circuitry underlying this food-sorting capability lies within the vagal lobe which dominates the medulla and constitutes over 20% of the brain volume in these species (Kotrschal and Palzenberger, 1992, Fig. 1A). The vagal lobe both receives the sensory input from the oropharynx and provides the motor output to the pharyngeal food-sorting organ. The VL thus contains elements homologous to both the nTS and nAmb, but arranged in a complex laminated system (Fig. 1B) (Morita et al., 1980; Morita and Finger, 1985; Finger, 1988, 2008). The sensory roots of the vagus nerve enter to form the white matter core of the lobe. The primary afferents turn radially outward from the fiber layer to terminate in the sensory layer which is equivalent to the vagal gustatory zone of the mid-caudal nTS (Fig. 1B, E) (Morita et al., 1980, Morita and Finger, 1985). The motor root of the vagus nerve originates from branchiomotor neurons deep to the central fiber layer and includes large motoneurons that innervate palatal organ muscle and gill arches. Since the primary afferent fibers end only in the sensory layer (Fig. 1E), and the motoneuron dendrites extend only to the upper part of the motor layer (Fig. 1D), there can be no direct contact between primary afferents and primary efferent populations. Theoretical considerations about the circuitry in this system are given in Finger (2008). Suffice it to say for the purposes of this contribution that neurons in the sensory layer project radially inward to end in the motor layer, thereby offering an anatomical basis for the existence of a reflex arc linking the sensory and motor

portions of the lobe (Goehler and Finger, 1992). Since this reflex system is organized topographically, we have suggested that these connections represent a reflex loop that permits fine motor control of the palatal organ permitting manipulation of fine food particles (Fig. 1C) (Morita et al., 1983; Goehler and Finger, 1992; Finger, 1988, 2008). As this elaborate neural system contains representations of the anterior pharynx of the fish, it is functionally equivalent, if not homologous to the interstitial and intermediate subnuclei of the nTS complex. The stereotypical anatomical arrangement of this structure in goldfish has facilitated study of the neurotransmitters and connectivity of the gustatory vagal reflex systems controlling pharyngeal motor activity leading to swallowing. In the present study, we tested whether a functional correlate exists to the connectivity observed in the anatomical studies, and offer pharmacological evidence that this reflex system utilizes glutamatergic activation of ionotropic glutamate receptors on the motoneurons to effect the reflex activation.

MATERIALS AND METHODS

Common goldfish, *Carassius auratus*, of both sexes ranging from 7 to 11.5 cm in standard length, were purchased from Hunting Creek Fisheries (Thurmont, MD). The animals were housed in a filtered and aerated aquarium at approximately 18˚C in the Animal Resources Center, University of Colorado Denver Health Sciences Center. All procedures reported herein were carried out with the approval of the University of Colorado Denver Health Sciences Center Institutional Animal Care and Use Committee.

Retrograde labeling of reflex interneurons

To retrogradely label the reflex interneurons in the sensory layer of the vagal lobe, biocytin injections were made into the motor layer in goldfish vagal lobe slices. Goldfish were cold anesthetized with ice and the brain was removed quickly from the skull. The brain was blocked in the transverse plane, and mounted on a platform with acrylate tissue glue (Vetbond, 3M, St. Paul, MN). The tissue was embedded in warmed 2% agarose (Type IX, melting point 8–17˚C; Sigma, St. Louis, MO), covered with chilled, oxygenated artificial cerebral spinal fluid (aCSF, 131 mM NaCl, 20 mM $NaCO_3$, 2 mM KCl, 1.25 mM KH_2PO_4, 2 mM $MgSO_4$, 2.5 mM $CaCl_2$, 10 mM dextrose, pH ~7.4), and sliced at 350 – 800 μm on a vibratome. After the sectioning, vagal lobe slices were put on the plastic petri dish and small crystal of biocytin (Sigma) were applied into the motor layer with a broken glass micropipette under microscopic observation. Brain slices were then incubated in the aCSF for 8–17 hours at room temperature and fixed with 4% paraformaldehyde in 0.1 M phosphate buffer (PB, pH 7.2) overnight. After rinsing in 20% sucrose in 0.1 M PB at 4˚C for 3–5 hours, the brain slices were embedded in 10% gelatin containing 20% sucrose and postfixed again in the same fixative containing 20% sucrose at 4˚C overnight. After washing in 20% sucrose in 0.1 M PB, the embedded brains were frozen and cut in the transverse plane at 36–40 μm on a cryostat. The sections were first washed in phosphate buffered saline (PBS) containing 0.3% Triton X-100 (PBST) for 30 minutes and then pretreated with 0.3% hydrogen peroxide (H_2O_2) in methanol for 10 minutes to reduce endogenous peroxidase. After 3 × 10 minutes washes in PBS, the sections were incubated in avidin-biotin HRP complex (1/200, Vector Laboratories, Burlingame, CA) for 1 hour at room temperature and washed 3 times in PBS (20 minutes each). Then the sections were incubated in 0.025% $NiCl_2$, 0.03% H_2O_2, 0.025% diaminobenzidine (DAB) in 0.1 M PB in the dark for 10 minutes and given 3 washes in PBS (10 minutes each). After washing, the sections were mounted on Superfrost Plus slides (Fisher, Fair Lawn, NJ) and dried overnight at room temperature. Then the mounted sections were counterstained with Giemsa, dehydrated in a graded series of ethyl alcohol, cleared with xylene, and coverslipped with Permount.

Double labeling of reflex interneurons (VRIs) and primary vagal afferent fibers

Double labeling was used to assess the relationship between VRIs and primary vagal afferent fiber terminals. The animals were anesthetized in 0.15 g/l MS-222 (tricaine methanesulfonate, Sigma), and then were placed in a fish surgical restraint to hold them stationary while permitting superfusion of the gills with aerated tap water containing 0.075 g/l MS-222. To expose the vagus nerve, a hole was made in the left side of the cranium just dorsal to the operculum. A small amount of cholera toxin subunit B conjugated Alexa Fluor 555 (Molecular Probes/Invitrogen, Eugene, OR) or 3,000 MW Texas Red or rhodamine-labeled fixable dextran amine (Molecular Probes/Invitrogen) was applied to the vagus nerve and the wound was covered with gelfoam (Upjohn, Kalamazoo, MI) and Vetbond Surgical Adhesive (3M Animal Care Products, St. Paul,. MN).

After 2–4 day survival, living vagal lobe slices were made as described above and observed under the fluorescent microscope to confirm labeling of primary afferent fibers and then biocytin was injected in the motor layer as described above. The slices were fixed and sectioned as above and the resulting tissue sections were incubated in PBST at 30 minutes. The fluorescent signals of cholera toxin, although apparent, were not sufficiently strong to permit visualization of all labeled processes. Therefore, sections were treated with immunohistochemistry with primary antiserum against cholera toxin subunit B (1/5000, polyclonal, produced against recombinant cholera toxin subunit B, Molecular Probes/Invitrogen) to optimize the signals. This antiserum produces no staining in uninjected goldfish. Sections were incubated in blocking solution (2% normal goat serum in PBST) for 2–5 hours at room temperature before incubation in primary antiserum for overnight at 4˚C. The sections then were washed in three changes of PBS (each 20 minutes) and incubated in Alexa 555 goat anti-rabbit IgG (1/1000) and streptavidin, Alexa Fluor 488 conjugate (1/2000, Molecular Probes/Invitrogen). After 3 washes with 0.1 M PB (each 20 minutes), the sections were mounted and coverslipped with Fluoromount-G (Southern Biotechnology Associates, Birmingham, AL).

Triple labeling of reflex interneuron terminals, vagal motoneurons, and calretinin

To label the vagal motoneurons, dextran tetramethylrhodamine and biotin (3,000 MW, micro-ruby, Molecular Probes/Invitrogen) was applied to the vagus nerve as mentioned above. Then a paste of dextran fluorescein and biotin (3,000 MW, micro-emerald, Molecular Probes/Invitrogen) was applied into the superficial portions of the vagal lobe to anterogradely label the axon terminals of the reflex interneurons. After 3 days survival, the animals were reanesthetized in 0.15 g/l MS-222 and perfused transcardially with teleost Ringer's solution followed by 4% paraformaldehyde in 0.1 M PB. The brains were removed from the skulls and postfixed in the same fresh fixative at 4˚C for 2–3 hours, then rinsed in 20% sucrose in 0.1 M PB at 4˚C for 2–5 hours. The brains were embedded in 10% gelatin containing 20% sucrose and postfixed as described above, and sectioned in the transverse plane at 32 μm on a cryostat. After preincubation in blocking solution, the sections were incubated in primary antisera against calretinin (1/4000, polyclonal, produced against recombinant human calretinin, Swant, Bellinzona, Switzerland) for 36 hours at 4˚C. The sections were then washed in three changes of PBS (each 20 minutes) and incubated in Cy-5 donkey-rabbit IgG (1/1000, Jackson Laboratories, West Grove, PA). After 3 washes in 0.1 M PB (20 minutes each), sections were coverslipped with Fluoromount-G.

Calcium imaging of vagal motoneurons

To label the vagal motoneurons with calcium sensitive dye, calcium green-1 dextran (CaGD, 10,000 MW, Molecular Probes/Invitrogen) was applied in vivo to the vagus nerve with the same surgical procedure described above. After 2–5 days survival, 300 μm brain slices of the vagal lobe were made by vibratome and set in the recording chamber. CaGD

fluorescence was observed by a fluorescence microscope (BX50WI, Olympus) equipped with 4x dry (NA 0.28) or 40x water (NA 0.80) objective lenses. Excitation illumination was by means of a xenon lamp with a band-pass excitation filter (460–500 nm), a dichroic mirror (505 nm), and an emission filter (510–560 nm). Fluorescence images were collected by CCD camera (MiCAM 02, Brain Vision, Japan) with a Videoscope VS4–1845 image intensifier. To evoke motoneuron responses from the reflex interneuron inputs, teflon-coated nichrome bipolar electrodes were placed on the sensory layer and single pulse (0.4 ms in duration) stimulation was applied. Optical images were obtained every 10 ms and total recording time was 2 s (200 frames). In order to obtain adequate baseline data, electrical stimulation was begun 800 ms after starting recording. One trial consisted of 3 rounds of electrical stimulation and recording with 30 seconds intervals. Fluorescence responses of each trial are shown as an average of the 3 recordings.

During the recordings, the chamber was superfused continuously with fresh-oxygenated aCSF at a flow rate of 1.5 ml/min. For pharmacological experiments for non-NMDA receptors, brain slices were incubated with aCSF containing 10 μM 6,7-dinitroquinoxaline-2,3-dione (DNQX, Sigma). To test the role of NMDA receptors, Mg^{2+}-free aCSF ($MgSO_4$ was omitted from normal aCSF) was perfused and 10 μM D(−)-2-amino-5-phosphoovaleric acid (AP-5, Sigma) was added to the Mg^{2+}-free aCSF.

The relative activation of motoneurons was expressed as ratio of the fractional changes in fluorescence intensity (ΔF/F). To permit quantitative inter-trial analysis, we measured peak of ΔF/F within 30 ms after electrical stimulation. In the pharmacological experiments, responses were normalized to control response prior to drug application. Paired, two-tailed Student's *t* tests were performed on responses from all pharmacological experiments to test the significance of the pharmacological treatments. $p < 0.01$ was considered significant.

Digital images

Brightfield photomicrographs were captured digitally on a SPOT RT camera (Diagnostic Instruments, Sterling Heights, MI) attached to on Olympus upright or dissection microscope. Fluorescent micrographs were captured by using an Olympus Fluoview confocal laser-scanning microscope. Digital images were then processed in Photoshop (Adove Systems, Mountain View, CA), adjusting only brightness, contrast, and color balance.

RESULTS

Morphology of vagal reflex interneurons

Following biocytin injections into the motor layer, many neurons were retrogradely labeled in the sensory zone (Fig. 2A, B). These labeled neurons project their axons to the motor layer, so they are implicated in the vagal reflex circuit; we termed these neurons as vagal reflex interneurons (VRIs). The somata of VRIs are distributed throughout the sensory layer, from the most superficial (layer II-III) to the deepest layers (layer XI). Regardless of soma position, the processes of the VRIs were nearly all oriented radially reaching through the layers of primary afferent termination (predominantly layers IV, VI and IX). In layer II-III, labeled VRI somata were round or pyriform and each extended a single dendrite radially inward. We identify these processes as dendrites since they taper somewhat over the first 30–50 μm as they descend. Some dendrites reached into deeper layers (layer IV-XI) and branched there (Fig. 2C). Cell deep in layer III also have lateral dendrites that ramify in layer IV (Fig. 3). In layers V and VII, some VRIs have a bipolar morphology (Fig. 2D) with dendrites extending radially both towards the surface and inward, reaching layers IV and XI (Fig. 2D). Some of the VRI neurons had a triangular shape cell body with an apical dendrite directed outward and basal dendrites extending inward (data not shown). In the deeper

portion of the sensory zone (layer IV-XI), most labeled neurons had round or tear drop shaped cell body with their major dendrites directed radially outward. Some of these deep neurons extended their dendrites to layer IV and branched there (Fig. 2E). In these deep layers, rare labeled neurons had a horizontally-oriented cell body with three or more primary dendrites running tangentially within the lobe (Fig. 2F).

Direct contact between primary vagal afferent fibers and vagal reflex interneuron

Previous studies showed that vagal primary afferent fibers terminated within layers IV, VI, and XI (Morita and Finger, 1985). As described above, some VRIs extend branched dendrites within these layers (Fig. 2C, D, E; Fig. 3). These features raised a possibility that some VRIs receive primary afferent inputs directly on their dendrites. To test this hypothesis, double labeling with 2 different tracers were performed. Dendritic branches of retrogradely labeled VRIs were prominent in the layers IV, VI and IX (Fig. 3A). After cholera toxin or dextran amine injections into the vagus nerve, numerous labeled terminal-like puncta were present within the layers of primary afferent termination: IV, VI, and IX only ipsilateral to the injection. In dextran-labeled cases, occasional primary afferent axons were filled completely allowing for better visualization. Confocal analysis revealed close apposition of VRI dendritic branches or somata and vagal primary afferent terminal in the layers IV and VI (Fig. 3B). On occasion, filled primary afferent fibers appeared to contact the somata of VRIs (Fig. 3C, D). In general however, direct contacts between primary afferents and labeled VRIs were not common. These results are consistent with our hypothesis, that some vagal afferent fibers directly contact the VRIs. It is likely that primary afferent terminals also synapse on the dendrites of non-VRIs which extend through the layers of primary afferent termination (Morita et al., 1980). Indeed the large majority of labeled puncta in any image are not apposed to labeled VRI dendrites even in areas where many VRIs have been retrogradely labeled.

Projections of vagal reflex interneurons to vagal motoneurons

Goehler and Finger (1992) utilized HRP to reveal the VRI projection into the motor layer of the vagal lobe, suggesting that VRIs make a synaptic contact with vagal motoneurons (Fig. 1C). However, microscopic observation with Nissl-stained sections showed that the motor layer contains not only large motoneurons, but also smaller neurons (Morita and Finger, 1985). Kainate-activated cobalt uptake experiments (Smeraski et al., 2001) and calcium binding protein immunohistochemistry (Ikenaga et al., 2006) also revealed the existence of two distinct populations of neurons in the vagal lobe motor layer. These two populations make clear sublayers, with motoneurons in the deeper sublamina while smaller neurons lie more superficially within the motor zone. These small, superficial neurons express GAD and so probably represent GABAergic interneurons (Anderson et al., 2002). The previous HRP study did not discriminate whether the axons of VRIs terminated onto the motoneurons, the smaller interneurons, or both. To test this, we employed triple fluorescent labeling with two different tracers and calretinin immunohistochemistry which labels the both small interneurons and motoneurons (Ikenaga et al., 2006; Huesa et al., 2008).

Following injection of fluorescent tracers into the sensory layers, many anterogradely labeled axon terminals occurred surrounding retrogradely labeled vagal motoneurons (Fig. 4A). Labeled axon terminals were more predominant in the outer motor layer than the inner one, as seen in previous HRP experiments (Goehler and Finger, 1992). With calretinin immunohistochemistry, we see two subpopulations of vagal motoneurons; outer ones are calretinin positive while inner motoneurons are negative (Ikenaga et al., 2006). In this study, both calretinin positive and negative vagal motoneurons received synaptic-like contacts from VRI axon terminals (Fig. 4B). In addition, in the outer layer of the vagal motor zone, there were close contacts between the calretinin-positive small interneurons neurons and

VRI axon terminals (Fig. 4C). These calreinin-positive small neurons can not be motoneurons because their size and location are different than the motoneurons which are retrogradely labeled by tracer injection into the nerve roots or palatal musculature. These results suggest that VRIs project both to the vagal motoneurons and to the small GABAergic interneurons in the motor layer.

Calcium imaging of goldfish vagal motoneurons

The above experiments showed the existence of a potential reflex arc between the sensory and motor layers of the goldfish vagal lobe. To study this reflex pathway physiologically, we utilized calcium imaging of vagal motoneurons in *in vitro* brain slices. Calcium green-1 dextran (CaGD) was injected into vagus nerve *in vivo* to retrogradely label the vagal motoneurons (Fig. 5A, B). In this way, only motoneurons were labeled with CaGD so any observed changes in the Ca^{++}-signal must arise from motoneurons, not from smaller interneurons. The stimulating electrode was placed on the sensory zone to directly stimulate the VRIs (Fig. 5A). A clear increase in intracellular Ca^{++} occurred in the motoneurons following the electrical stimulation of the sensory layer (Fig. 5C1). These responses were suppressed when the brain slices were superfused with Ca^{2+}-free aCSF (Fig. 5C2) indicating that influx of extracellular Ca^{++} was a necessary component of these responses. These results support the histological findings of the existence of reflex projections from the sensory to motor layers.

To verify our hypothetical reflex circuit, we tested whether cutting between the stimulating (sensory layer) electrode and the motor layer would eliminate the increase in Ca^{++}. For these experiments (n=3), the stimulating electrode first was placed on the sensory layer and motor layer responses were verified (Fig. 5D). The stimulating electrode was removed and a small scissors was used to transect the fiber layer between the sensory and motor layers. When the stimulating electrode was replaced in its original location, no responses were seen from the motor layer although calcium changes around stimulating electrode were still observed (Fig. 5E). Thus electrical stimulation of the sensory zone evokes Ca^{++} influx into underlying motoneurons via a radially-organized reflex pathway consistent with that described anatomically.

Point-to-point organization of the vagal reflex system

Local injections of tracer in the VL sensory layer result in a topographically-ordered projection to the motor layer, suggesting that the orotopic organization is maintained within the reflex arc (Goehler and Finger, 1992). In this study, we tried to verify this topographic organization of the vagal reflex circuit with the converse method, microinjecting a retrograde tracer into the motor layer. When biocytin injections were restricted to the dorsal portion of the motor layer (Fig. 6A1), labeled VRIs occur only in the dorsal part of the sensory layer (Fig. 6A2), not ventrally (Fig. 6A3). Similarly ventral tracer injections labeled VRIs only in the ventral sensory layer (Fig. 6B), thus confirming the original description.

We utilized calcium imaging in 4 slices to test whether a functional correlate existed to this anatomically-defined vagal reflex circuit. When the stimulating electrode was placed onto the dorsal sensory layer, calcium responses were elicited only from the dorsal motor layer (Fig. 6C). When the stimulating electrode was moved to the ventral sensory layer, calcium changes were seen in the ventral portion of the motor layer (Fig. 6D).

Taken together the present results suggest that the sensory-motor orotopy in the goldfish vagal lobe is also maintained within the reflex arc. This supports the hypothesis that this point-to-point reflex system may underlie the ability of the fish to sort fine particulate matter according to chemosensory cues (Finger, 2008).

AMPA/kainate receptors on the vagal motoneurons

In the goldfish vagal lobe, vagal motoneurons are labeled by kainate-activated cobalt uptake, suggesting that these motoneurons possess calcium-permeable AMPA/kainate receptors (Smeraski et al., 2001; Ikenaga et al., 2006). In order to test whether the VRI input to the motoneurons involves a glutamatergic system, we combined calcium imaging with pharmacological manipulations using antagonists for AMPA/kainate receptors.

To avoid stimulating interneurons and primary afferents of the sensory layer in these slice experiments, the sensory layer was cut off and the stimulating electrode was placed in the fiber layer to directly stimulate axons of VRIs (Fig. 7A). In this preparation, as in the previous experiments entailing stimulation of the sensory layers, calcium changes occurred in the vagal motoneurons following electrical stimulation. These responses were suppressed by incubation in Ca^{2+}-free aCSF (data not shown). Vagal motoneuron calcium responses were significantly abolished by application of a selective non-NMDA receptor antagonist, DNQX (10 μM, 22.3 ± 16.3% of control level, Fig. 7B, C). This suppression was significantly reversible, recovering to, 68.7 ± 23.4% of control values 30–45 min after washout of the drug.

Effects of NMDA receptor on the vagal motoneurons

The involvement of NMDA receptors in the neurotransmission of vagal reflex systems was also tested with calcium imaging since AMPA/kainate receptor antagonists did not completely eliminate vagal motoneuron calcium responses (Fig 7B). The amplitudes of the vagal motoneuron Mg^{2+}-free aCSF (454.6 ± 131.4% of control level, Fig. 8A, B) suggesting participation by NMDA receptors. By application of 10 μM AP-5, a competitive NMDA receptor antagonist, these enhanced responses were significantly suppressed (57.6 ± 33.7% of control level), although small responses remained. Following wash out of AP-5 under Mg^{2+}-free conditions (15–30 min), the original synaptic enhancement partially recovered (382.9 ± 184.2% of control level). To test whether AMPA/kainate receptors are implicated in the responses remaining after exposure to AP-5, we sequentially added two antagonists, AP-5 and then DNQX, in Mg^{2+}-free aCSF. The responses remaining after 10μM AP-5 alone (104.1 ± 52.1% of control level) were significantly suppressed with 10μM DNQX application (35.9 ± 31.7%, Fig. 9A, B). These experiments suggest that both non-NMDA and NMDA glutamate receptors underlie synaptic transmission from VRIs to vagal motoneurons. Whether the increases in intracellular Ca^{2+} that we observe are due to influx through Ca-permeable glutamate receptors or through voltage-gated Ca-channels following spike initiation could not be determined in these experiments. Nonetheless, the time course and fast rise-time of the Ca^{++} responses we observe are consistent with those generated by single action potentials in pyramidal neurons of cortex (Smetters et al., 1999).

DISCUSSION

When appetitive food items activate the taste buds of the posterior pharynx, the deglutive motor network in the medulla is activated to produce a complex pattern of activity in the oropharyngeal musculature to drive the food bolus into the esophagus (Jean, 2001). The afferent limb of this reflex system relays in the nTS to trigger a solitario-ambigual circuit (Bieger, 1991; Lu and Bieger, 1998). This reflex network linking gustation to ingestion is especially elaborate in goldfish which possess a specialization of the pharynx enabling them to manipulate and sort potential food items in the rostral pharynx (Finger, 2008). This reflex network linking vagal gustatory afferents to pharyngeal motoneurons appears to be a common, and therefore evolutionarily ancient, vertebrate trait. The present study examined in goldfish the neurotransmitters and receptors employed by the obligatory interneuronal network bridging the afferent and efferent limbs of this reflex system. We find that

ionotropic glutamate receptors – both AMPA/kainate and NMDA – are essential for this linkage. Also we find that in keeping with previous anatomical descriptions for this system (Goehler and Finger, 1992), the reflex system is organized functionally in a topographically-organized fashion within the vagal lobe consistent with its function in intraoral food-sorting. Figure 10 summarizes the current findings in the context of our previous results concerning neurotransmitters in this system. Both the primary afferent fibers and the VRIs utilize glutamate as the principal neurotransmitter which activates both AMPA/kainate and NMDA type receptors in both synaptic systems.

The vagus nerve serves as both the afferent and efferent limb for a variety of reflexes. General visceral information from cardiovascular, pulmonary, and gastrointestinal sensors trigger autonomic reflexes mediated by preganglionic parasympathetic neurons of the dorsal motor nucleus of the vagus. Conversely, mechanosensory and chemosensory inputs from the oropharynx trigger reflex systems which largely activate nAmb and other branchiomotor muclei via the perisolitary medullary reticular formation (Jean, 2001). Although the nTS serves as the primary sensory nucleus for all these vagal inputs, the nTS is divisible into numerous subnuclei each serving a distinct subsystem (Katz and Karten, 1983; Altschuler et al., 1989) and maintaining a unique pattern of connectivity (Powley, 2000). Nonetheless, glutamate, acting on ionotropic glutamate receptors, is the key neurotransmitter of primary afferents for both the gustatory (Bradley et al., 1996; Li and Smith, 1997; Smeraski et al., 1998; Smith et al., 1998; Ikenaga et al., 2007) and general visceral afferents (Andresen and Yang, 1990; Aylwin et al., 1997; Lu and Bieger, 1998).

The caudal nTS receives inputs from the branches of the vagus nerve that innervates gastrointestinal as well as cardiovascular and respiratory organs. Reflexes originating in this region largely activate the preganglionic parasympathetic neurons of the dorsal motor nucleus of the vagus, but often do so with no obligatory interneuron. That is, primary general visceral afferent fibers terminate directly on dendrites of neurons in the dorsal motor nucleus (Powley, 2000). Of course higher-order reflex systems exist for both rostral and caudal nTS, but rostral nTS, which is far removed from the dorsal motor nucleus of the vagus, offers less opportunity for the monosynaptic reflex connections than caudal nTS. Nonetheless, collaterals of the gustatory primary afferents terminate in the vicinity of the dendrites of the preganglionic parasympathetic neurons of the salivatory nuclei suggesting the possibility of monosynaptic connections for this preganglionic population (Bradley et al., 1980; Kim et al., 2008). Thus the 2-neuron reflex arc appears to be the shortest path underlying many autonomic reflexes although longer loops also occur.

In contrast, reflex systems involving branchiomotor musculature instead utilize a 3-neuron minimum reflex arc with one or more obligatory interneurons bridging between primary sensory input and motor output. In rodents, cells in the esophageal region of the nTS (subnucleus centralis) projects to esophageal motorneurons of nAmb (Bao et al., 1995; Cunningham and Sawchenko, 2000). Likewise, a 3- or 4-neuron reflex system connects the rostral nTS to motoneurons for lingual and orofacial motoneurons as originally proposed by Ramon y Cajal (Jean, 2001; Bradley and Kim, 2006). The minimum 3-neuron reflex arc is more a characteristic of oral and oropharyngeal regions of the nTS but not of general visceral, caudal regions of the same nucleus. Our anatomical findings in the current paper are consonant with a 3 neuron reflex arc from gustatory input to pharyngeal motoneurons, i.e. the minimum path length for this reflex entails an obligatory interneuron between the primary afferents and the motoneurons.

Although several histological studies examine the solitario-ambigual reflex circuit in mammals, information about physiological aspects and neurotransmitters are limited. Most studies focus on the specialized circuitry for the upper esophagus (Wang et al., 1991a; Lu

and Bieger, 1998). This circuit, which is readily identifiable by somatostatin immunoreactivity in mammals (Cunningham and Sawchenko, 1989) lies fortuitously within the brainstem to make it amenable to a slice preparation (Wang et al., 1991a, b) facilitating studies on the neuropharmacology and neurotransmitters of the system. Unfortunately, similar preparations embracing gustatory components of the nucleus solitarius and branchiomotor nuclei in mammals are not feasible. The elongate, complex structure of nTS and the distributed nature of the oropharyngeal motor nuclei make reflex systems between these structures difficult for physiological study especially in *in vitro* slices.

In contrast, the large size and stereotypical organization of the vagal lobe in goldfish greatly facilitate study of gustato-pharyngeal reflex systems. Because all elements of the circuit lie within a single transverse plane, it is feasible to utilize an in vitro slice preparation to characterize the connectivity and neurotransmitters in this system (Finger and Dunwiddie, 1992; Smeraski et al., 1999; Sharp and Finger, 2002). Primary gustatory afferent fibers utilize glutamate acting via AMPA/kainate and NMDA receptors to excite second-order neurons in the lobe (Smeraski et al., 1999). Here we show that the VRI also rely on glutamatergic synapses to activate ionotropic glutamate receptors on the pharyngeal motoneurons. The heavy reliance on glutamatergic transmission in this reflex system is thus similar in goldfish and in the solitario-ambigual linkage in rodents (Wang et al., 1991a).

Reflex systems from the nTS in mammals reaching both preganglionic parasympathetic (Neff et al., 1998; Bradley and Kim, 2006) and branchiomotor nuclei (Hayakawa et al., 2000) also appear to rely on glutamate as one of the principal neurotransmitters. In addition, GABAergic interneurons of the nTS also project to branchiomotor nuclei (Hayakawa et al 2000) which possess GABAA receptors (Yajima et al., 1997). Whether a similar GABAergic reflex system exists in the goldfish is unclear. We do find that the reflex system impacts on both GABAergic interneurons and the primary motoneurons of the vagal motor layer (nAmb equivalent). Hence participation of GABAegic elements in the reflex circuitry is common to both fish and mammals.

Previous anatomical studies on the vagal lobe show that the large majority of neurons in the sensory layer are unipolar or bipolar neurons with radially directed dendrites passing through the layers of termination of the primary gustatory afferents. Many of these neurons possess Ca^{++}-permeable AMPA/kainate receptors (Smeraski et al., 2001) and express one or both of the calcium binding proteins (CaBP) calbindin or calretinin (Huesa et al., 2008). Many of these CaBP-expressing neurons appear to participate in the vagal reflex system since fascicles of CaBP-immunoreactive fibers extend radially inward, bridging between the sensory and motor layers of the lobe. Since tracer injections in the sensory layers do not retrogradely label neurons in the motor layer, the radially-oriented CaBP+ fibers must originate from neurons of the sensory layer and represent axons of the VRI neurons investigated in the present report. We find no evidence for peptide immunoreactivity in these interneurons (Farrell et al., 2002) and therefore do not equate them with the somatostatin containing vagal reflex neurons implicated in control of esophageal reflexes in mammals (Cunningham and Sawchenko, 1989). Rather, the system in goldfish appears functionally and anatomically equivalent to the reflex system mediated by the superior laryngeal nerve (Kitagawa et al., 2002).

We found that both AMPA/kainate and NMDA receptors are involved in the linkage from the reflex interneuron to the branchiomotor neurons. Similarly both NMDA and non-NMDA ionotropic glutamate receptors participate in solitario-ambiguual activation of oesophageal and cardiac motoneurons in mammals (Wang et al., 1991a; Neff et al., 1998). Thus our study extends to the gustatory modality neurons the complex glutamatergic receptor systems previously described for the viseromotor reflex systems.

Acknowledgments

The authors thank Dr. Diego Restrepo for graciously permitting use of the equipment for calcium imaging and Rob Hallock for useful comments on drafts of this manuscript.

Supporting grant information: National Institutes of Health grants PO1 DC00147 (T.E.F), and P30 DC04657 (D. Restrepo & T.E.F., co-P.I.).

LITERATURE CITED

Altschuler SM. Laryngeal and respiratory protective reflexes. Am J Med. 2001; 111 Suppl 8A 90S–94S.

Altschuler SM, Bao XM, Bieger D, Hopkins DA, Miselis RR. Viscerotopic representation of the upper alimentary tract in the rat: sensory ganglia and nuclei of the solitary and spinal trigeminal tracts. J Comp Neurol. 1989; 283:248–268. [PubMed: 2738198]

Anderson K, Böttger B, Lariviere K, Trudeau V, Finger TE. Gabaergic cells in the goldfish vagal lobe. Chem Senses. 2002; 27:A110.

Andresen MC, Yang MY. Non-NMDA receptors mediate sensory afferent synaptic transmission in medial nucleus tractus solitarius. Am J Physiol. 1990; 259(Pt 2):H1307–H1311. [PubMed: 1977326]

Atema J. Structures and functions of the sense of taste in the catfish (*Ictalurus natalis*). Brain Behav Evol. 1971; 4:273–294. [PubMed: 5118142]

Aylwin ML, Horowitz JM, Bonham AC. NMDA receptors contribute to primary visceral afferent transmission in the nucleus of the solitary tract. J Neurophysiol. 1997; 77:2539–2548. [PubMed: 9163375]

Bao H, Bradley RM, Mistretta CM. Development of intrinsic electrophysiological properties in neurons from the gustatory region of rat nucleus of solitary tract. Brain Res Dev Brain Res. 1995; 86:143–154.

Barrett RT, Bao X, Miselis RR, Altschuler SM. Brain stem localization of rodent esophageal premotor neurons revealed by transneuronal passage of pseudorabies virus. Gastroenterology. 1994; 107:728–737. [PubMed: 8076758]

Bieger D. Neuropharmacologic correlates of deglutition: lessons from fictive swallowing. Dysphagia. 1991; 6:147–164. [PubMed: 1680608]

Bradley RM, Cheal ML, Kim YH. Quantitative analysis of developing epiglottal taste buds in sheep. Journal of Anatomy. 1980; 130:25–32. [PubMed: 7364661]

Bradley, RM.; Kim, M. Reflex Connections. In: Bradley, RM., editor. The Role of the Solitary Tract in Gustatory Processing. Boca Raton: CRC Press; 2006. p. 67-82.

Bradley RM, King MS, Wang L, Shu X. Neurotransmitter and neuromodulator activity in the gustatory zone of the nucleus tractus solitarius. Chem Senses. 1996; 21:377–385. [PubMed: 8670717]

Callan WT, Sanderson SL. Feeding mechanisms in carp: crossflow filtration, palatal protrusions and flow reversals. J Exp Biol. 2003; 206:883–892. [PubMed: 12547943]

Cunningham ET Jr, Sawchenko PE. A circumscribed projection from the nucleus of the solitary tract to the nucleus ambiguus in the rat: anatomical evidence for somatostatin-28-immunoreactive interneurons subserving reflex control of esophageal motility. J Neurosci. 1989; 9:1668–1682. [PubMed: 2470875]

Cunningham ET Jr, Sawchenko PE. Dorsal medullary pathways subserving oromotor reflexes in the rat: implications for the central neural control of swallowing. J Comp Neurol. 2000; 417:448–466. [PubMed: 10701866]

Farrell WJ, Bottger B, Ahmadi F, Finger TE. Distribution of cholecystokinin, calcitonin gene-related peptide, neuropeptide Y, and galanin in the primary gustatory nuclei of the goldfish. J Comp Neurol. 2002; 450:103–114. [PubMed: 12124755]

Finger TE. Sensorimotor mapping and oropharyngeal reflexes in goldfish, *Carassius auratus*. Brain Behav Evol. 1988; 31:17–24. [PubMed: 3334903]

Finger TE. Sorting food from stones: the vagal taste system in goldfish, *Carassius auratus*. J Comp Physiol A Neuroethol Sens Neural Behav Physiol. 2008; 194:135–143. [PubMed: 18228077]

Finger TE, Dunwiddie TV. Evoked responses from an in vitro slice preparation of a primary gustatory nucleus: the vagal lobe of goldfish. Brain Res. 1992; 580:27–34. [PubMed: 1504805]

Goehler LE, Finger TE. Functional organization of vagal reflex systems in the brain stem of the goldfish, *Carassius auratus*. J Comp Neurol. 1992; 319:463–478. [PubMed: 1619041]

Hayakawa T, Zheng JQ, Yajima Y. Direct synaptic projections to esophageal motoneurons in the nucleus ambiguus from the nucleus of the solitary tract of the rat. J Comp Neurol. 1997; 381:18–30. [PubMed: 9087416]

Hayakawa T, Zheng JQ, Seki M, Yajima Y. Synaptology of the direct projections from the nucleus of the solitary tract to pharyngeal motoneurons in the nucleus ambiguus of the rat. J Comp Neurol. 1998; 393:391–401. [PubMed: 9548557]

Hayakawa T, Takanaga A, Maeda S, Ito H, Seki M. Monosynaptic inputs from the nucleus tractus solitarii to the laryngeal motoneurons in the nucleus ambiguus of the rat. Anat Embryol (Berl). 2000; 202:411–420. [PubMed: 11089932]

Huesa G, Ikenaga T, Bottger B, Finger TE. Calcium-fluxing glutamate receptors associated with primary gustatory afferent terminals in goldfish (*Carassius auratus*). J Comp Neurol. 2008; 506:694–707. [PubMed: 18067143]

Ikenaga T, Huesa G, Finger TE. Co-occurrence of calcium-binding proteins and calcium-permeable glutamate receptors in the primary gustatory nucleus of goldfish. J Comp Neurol. 2006; 499:90–105. [PubMed: 16958099]

Ikenaga T, Ogura T, Finger TE. Neurotransmitters in brainstem gustatory reflex circuitry. Chem Senses. 2007; 32:A44.

Jean A. Brain stem control of swallowing: neuronal network and cellular mechanisms. Physiol Rev. 2001; 81:929–969. [PubMed: 11274347]

Katz DM, Karten HJ. Visceral representation within the nucleus of the tractus solitarius in the pigeon, *Columba livia*. J Comp Neurol. 1983; 218:42–73. [PubMed: 6886066]

Kessler JP. Involvement of excitatory amino acids in the activity of swallowing-related neurons of the ventro-lateral medulla. Brain Res. 1993; 603:353–357. [PubMed: 8096425]

Kim M, Chiego DJ Jr, Bradley RM. Ionotropic glutamate receptor expression in preganglionic neurons of the rat inferior salivatory nucleus. Auton Neurosci. 2008; 138:83–90. [PubMed: 18096442]

Kitagawa J, Shingai T, Takahashi Y, Yamada Y. Pharyngeal branch of the glossopharyngeal nerve plays a major role in reflex swallowing from the pharynx. Am J Physiol Regul Integr Comp Physiol. 2002; 282:R1342–R1347. [PubMed: 11959674]

Kotrschal K, Palzenberger M. Neuroecology of cyprinids: comparative, quantitative histology reveals diverse brain patterns. Environ. Biol. Fishes. 1992; 33:135–152.

Lamb CF, Finger TE. Gustatory control of feeding behavior in goldfish. Physiol Behav. 1995; 57:483–488. [PubMed: 7753885]

Li CS, Smith DV. Glutamate receptor antagonists block gustatory afferent input to the nucleus of the solitary tract. J Neurophysiol. 1997; 77:1514–1525. [PubMed: 9084616]

Lu WY, Bieger D. Vagal afferent transmission in the NTS mediating reflex responses of the rat esophagus. Am J Physiol. 1998; 274(Pt 2):R1436–R1445. [PubMed: 9612412]

Miller AJ. Oral and pharyngeal reflexes in the mammalian nervous system: their diverse range in complexity and the pivotal role of the tongue. Crit Rev Oral Biol Med. 2002; 13:409–425. [PubMed: 12393760]

Morita Y, Finger TE. Reflex connections of the facial and vagal gustatory systems in the brainstem of the bullhead catfish, *Ictalurus nebulosus*. J Comp Neurol. 1985; 231:547–558. [PubMed: 3968255]

Morita Y, Ito H, Masai H. Central gustatory paths in the crucian carp, *Carassius carassius*. J Comp Neurol. 1980; 191:119–132. [PubMed: 7400389]

Neff RA, Mihalevich M, Mendelowitz D. Stimulation of NTS activates NMDA and non-NMDA receptors in rat cardiac vagal neurons in the nucleus ambiguus. Brain Res. 1998; 792:277–282. [PubMed: 9593939]

Powley TL. Vagal circuitry mediating cephalic-phase responses to food. Appetite. 2000; 34:184–188. [PubMed: 10744908]

Sharp AA, Finger TE. GABAergic modulation of primary gustatory afferent synaptic efficacy. J Neurobiol. 2002; 52:133–143. [PubMed: 12124751]

Sibbing FA, Uribe R. Regional specializations in the oropharyngeal wall and food processing in the carp (*Cyprinus carpio* L.). Neth J Zool. 1985; 35:377–422.

Sibbing FA, Osse JMW, Terlouw A. Food handling in the carp (*Cyrinus carpio*): its movement patterns, mechanisms, and limitations. J Zool. 1986; 210:161–203.

Smeraski CA, Dunwiddie TV, Diao LH, Magnusson KR, Finger TE. Glutamate receptors mediate synaptic responses in the primary gustatory nucleus in goldfish. Abstr Soc Neurosci. 1996:22.

Smeraski CA, Dunwiddie TV, Diao L, Finger TE. Excitatory amino acid neurotransmission in the primary gustatory nucleus of the goldfish *Carassius auratus*. Ann N Y Acad Sci. 1998; 855:442–449. [PubMed: 10049227]

Smeraski CA, Dunwiddie TV, Diao L, Finger TE. NMDA and non-NMDA receptors mediate responses in the primary gustatory nucleus in goldfish. Chem Senses. 1999; 24:37–46. [PubMed: 10192474]

Smeraski CA, Bottger B, Finger TE. Kainate-activated cobalt uptake in the primary gustatory nucleus in goldfish: visualization of the morphology and distribution of cells expressing AMPA/kainate receptors in the vagal lobe. J Comp Neurol. 2001; 431:59–74. [PubMed: 11169990]

Smetters D, Majewska A, Yuste R. Detecting action potentials in neuronal populations with calcium imaging. Methods. 1999; 18:215–221. [PubMed: 10356353]

Smith DV, Li CS, Davis BJ. Excitatory and inhibitory modulation of taste responses in the hamster brainstem. Ann N Y Acad Sci. 1998; 855:450–456. [PubMed: 9929638]

Wang YT, Bieger D, Neuman RS. Activation of NMDA receptors is necessary for fast information transfer at brainstem vagal motoneurons. Brain Res. 1991a; 567:260–266. [PubMed: 1667902]

Wang YT, Neuman RS, Bieger D. Somatostatin inhibits nicotinic cholinoceptor mediated-excitation in rat ambigual motoneurons in vitro. Neurosci Lett. 1991b; 123:236–239. [PubMed: 1674125]

Yajima Y, Hayakawa T, Hayashi Y. Evidence for GABAA receptor-mediated inhibition in ambiguous motoneurons. Acta Otolaryngol. 1997; 532 Suppl:132–134.

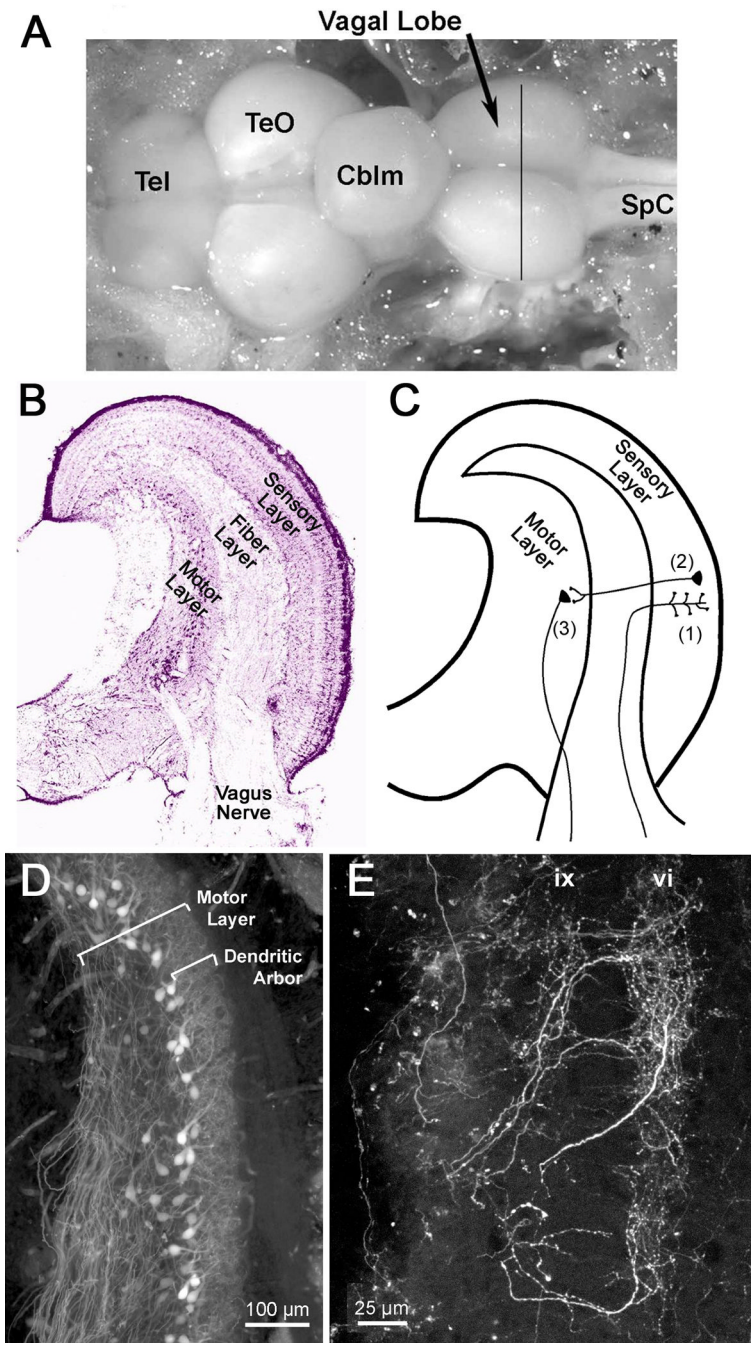

Figure 1.

Anatomy and circuitry of the vagal lobe. **A:** Dorsal view of the exposed goldfish brain; anterior to the left. The solid vertical line indicates the level of the section shown in B (data from Huesa et al., 2008). Cblm, cerebellum; Tel, telencephalon; TeO, optic tectum; SpC, spinal cord. **B:** Nissl stained transverse goldfish vagal lobe. The lobe is divisible into three main layers: superficial sensory layer, central fiber layer, and deeper motor layer. **C:** Hypothesized vagal reflex circuit for the goldfish food sorting behavior. Gustatory information from taste buds of oral cavity (palatal organ and gill arches) is conveyed by the vagus nerve through the fiber layer and terminates in the sensory layer (1). Vagal primary afferent fibers activate vagal reflex interneurons (VRIs) which project through the fiber

layer (2) and terminate on the vagal motoneurons (3). These motoneurons innervate muscles of the palatal organ and activate them to manipulate food particles in the oral cavity. **D:** Micrograph showing retrogradely labeled motor neurons and their dendritic ramifications in the superficial part of the motor layer following labeling of the nerve root with rhodamine dextran. The motor layer in the same orientation as panel B. **E:** Confocal micrograph of the sensory layers following filling with rhodamine dextran of a few primary afferent fibers from the palatal organ. Each fiber terminates in a restricted domain of either layer vi with some collateral endings in layer ix. No primary afferent fibers terminate in the motor layer.

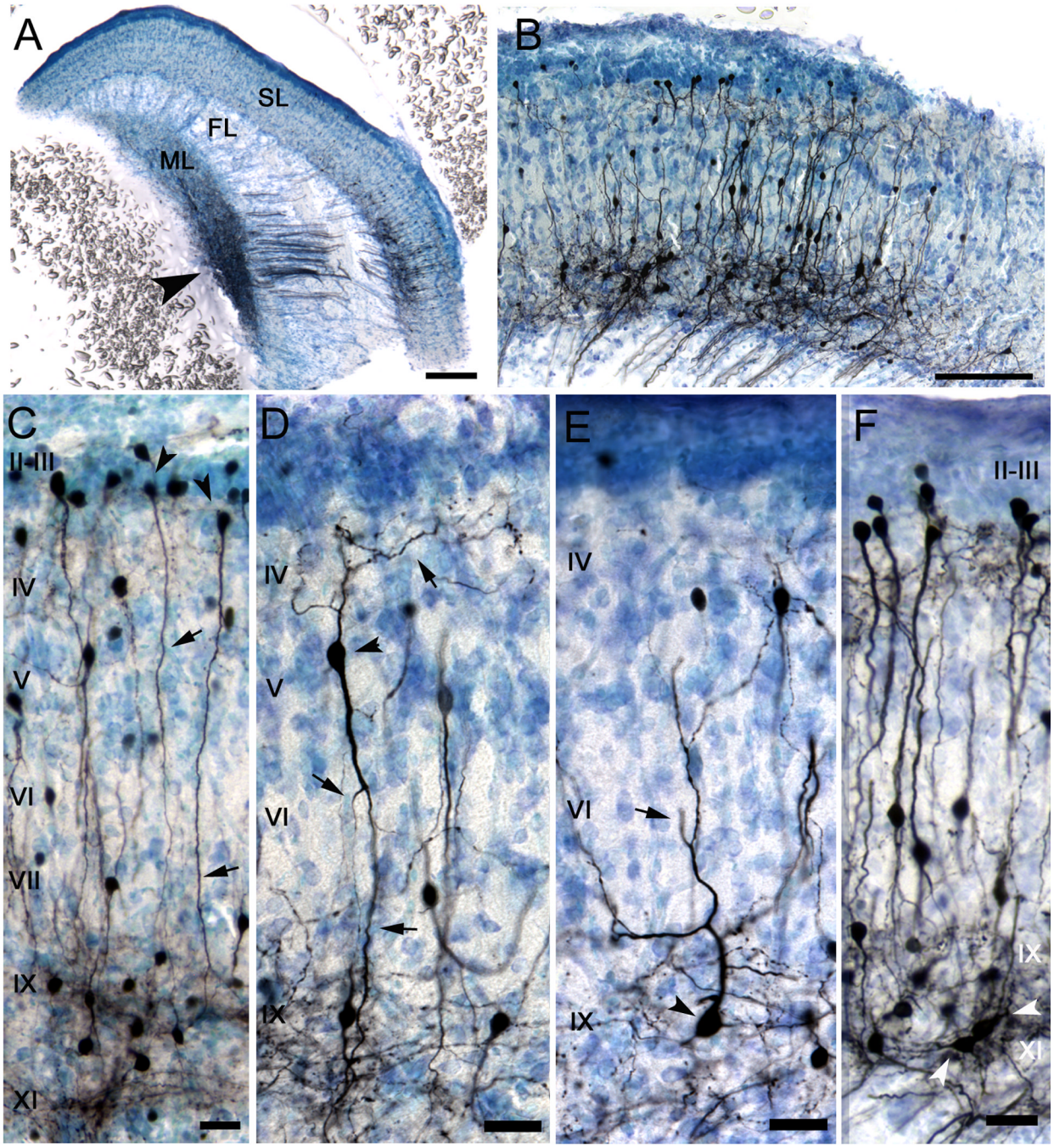

Figure 2.

Micrographs of VRIs retrogradely labeled with biocytin injected into the middle portion of the motor layer and visualized with DAB. **A:** Biocytin was injected into middle portion of motor layer (arrowhead, ML). Labeled axons (arrow) run across the fiber layer (FL) and neuronal somata are labeled retrogradely in sensory layer (asterisk, SL). **B:** Higher magnification picture indicated with an asterisk in A. Retrogradely labeled somata are distributed throughout the sensory layer. Most VRIs have round or spindle shape soma and extend dendrites radially inward and outward. Few cells have tangentially-oriented processes. **C–F:** Higher magnification images of retrogradely labeled VRIs. Primary afferent fibers terminate in layers IV, VI and IX (Morita and Finger, 1985). **C:** Unipolar

neurons in Layer III (arrowheads) extend their basal dendrites to layer IX (arrows). **D:** Bipolar neuron in layer V (arrowhead) extends its dendrites both inward and outward. Dorsal dendrite branches in layer IV and ventral one in layers VI and IX (arrows). **E:** Unipolar neuron in layer IX (arrowhead) directs its dendrite outward and branch in the layers IV and VI (arrow). **F:** Rare neurons in layer IX showed multipolar somata and possess a dendrite oriented tangentially (white arrows). Scale Bar = 200 μm (A), 50 μm (B), 20μm (C–F).

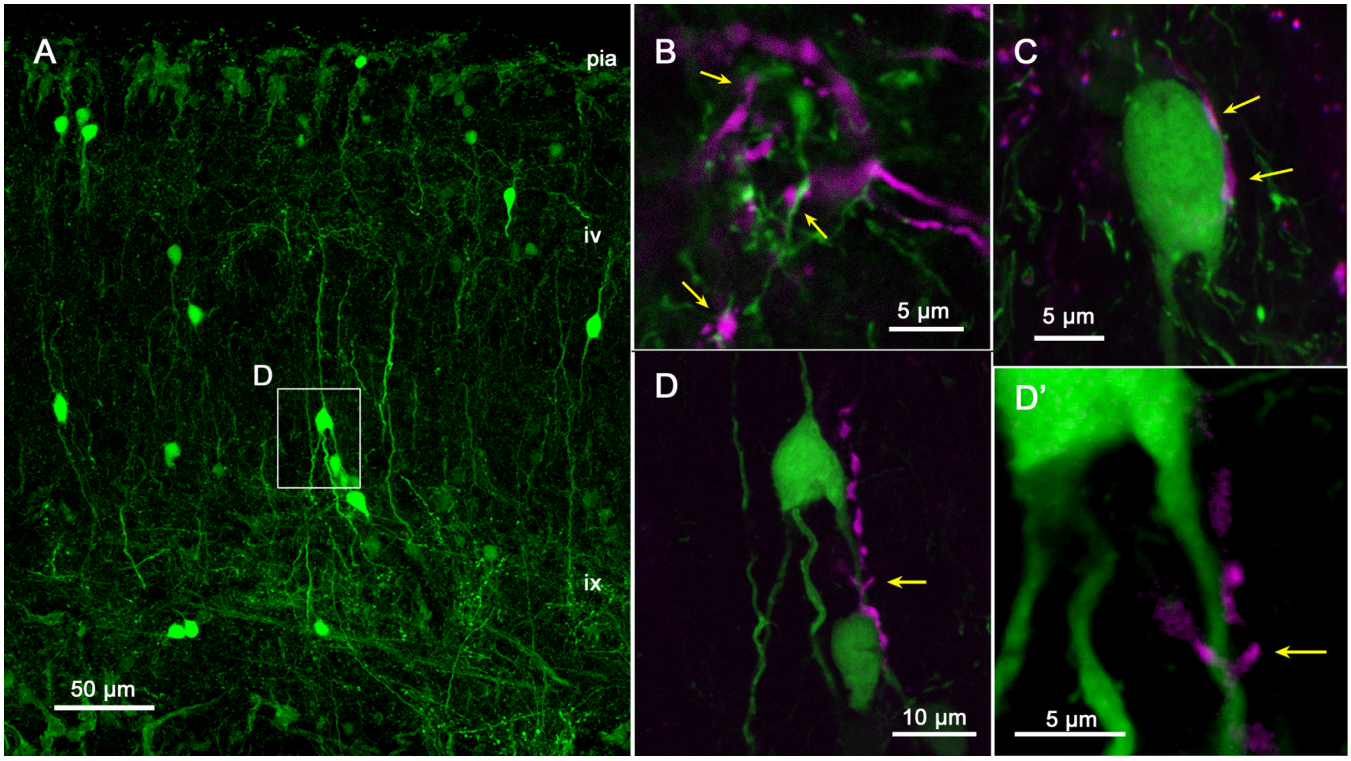

Fig. 3.

A Micrograph of a VRIs in the sensory layers of the vagal lobe retrogradely labeled (green) by a biocytin injection into the motor layer. As shown in the previous figure, retrogradely labeled neurons are present in superficial, middle and deep layers of the sensory layers but dendrites ramify mostly within layers ix and vi, two layers of termination of primary afferent fibers. Box D shows the area enlarged in panels **D** and **D'**. Scale bar = 50 µm. **B**. Confocal image through the neuropil of layer vi in a different section than that shown in A. The arrows indicate several points of apparent contact between the primary afferent fibers (magenta) and the dendrites (green) of the retrogradely labeled VRI neurons. **C**. Z-stack confocal image (14 @ 0.25 µm = 3.25µm thickness) showing a VRI cell body in layer vi apparently being contacted by a labeled primary afferent fiber (magenta). **D**. Small z-stack confocal image (14 @ 0.25 µm = 3.25µm thickness) showing close apposition between labeled primary afferent fiber (magenta) and two retrogradely labeled VRIs (green). The area indicated by the arrow is shown enlarged in a single plane confocal image in **D'**.

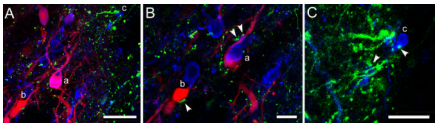

Figure 4.

A: Micrographs showing triple labeling with micro-ruby labeled vagal motoneurons (red), biocytin labeled VRI axon terminals (green), and calretinin immunohistochemistry (blue) in the motor layer. Calretinin marks two distinct cell populations (Ikenaga et al., 2006). Small calretinin-positive, micro-ruby-negative neurons (c) are GABAergic interneurons of the superficial part of the motor layer. Calretinin-positive motoneurons (a) are magenta and represent a subset of the motoneuronal population. This picture is stack of 10 confocal images spaced by 1 μm. **B:** Higher magnification single confocal image plane showing neurons a and b from panel A. Green-labeled puncta from VRIs appear to contact the somata of both outer (calretinin-positive) and inner (calretinin-negative) motoneurons. **C:** Apparent synaptic contact between calretinin positive smaller interneuron (c) and VRIs terminals (arrow) is observed. Scale bar = 50 μm (A), 20 μm (B, C).

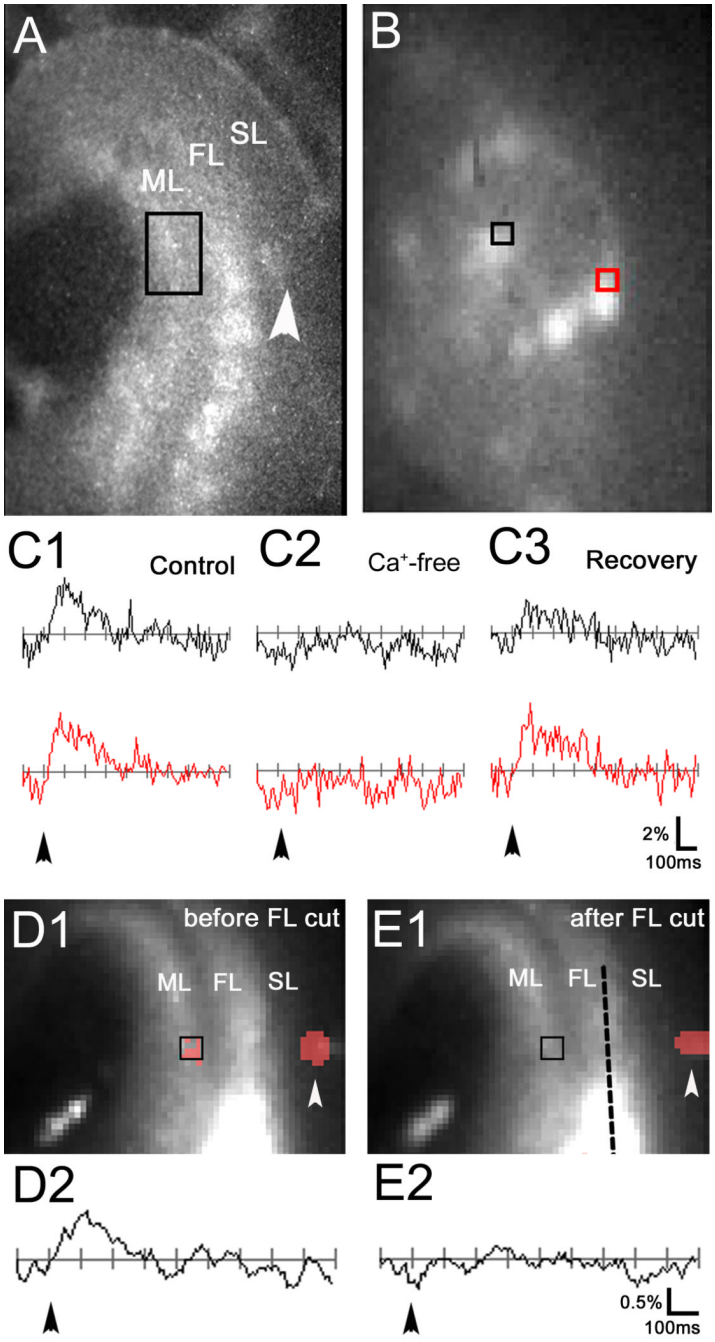

Figure 5.

Calcium imaging with vagal motoneurons shows the existence of a reflex pathway from sensory to motor layers. Compare this image with Fig. 1B, C. **A:** Injections of the calcium sensitive dye, calcium green dextran, into the vagus nerve retrogradely label vagal motoneurons visible as bright spots of the motor layer (ML) in this in vitro vagal lobe slice preparation. The stimulating electrode was placed into the sensory layer (SL, white arrowhead). Bright fluorescence also is visible in fascicles of fibers within the fiber layer (FL) between the black rectangle and the white arrowhead. **B:** Higher magnification image indicated as a rectangle in panel A. Individual labeled motoneurons can be distinguished clearly. **C1–3:** Graphs of intracellular calcium responses of the vagal motoneurons. Each

black and red trace represents the signals obtained from the regions of interest indicated as black and red squares in B respectively. In normal aCSF (**C1**), intracellular calcium levels increased following the electrical stimulation (arrowhead, left). These responses were suppressed in Ca^{2+}-free aCSF (**C2**) and recovered in normal aCSF (**C3**). **D, E:** Effect of cutting the fiber layer (FL) between the sensory layer where the stimulating electrode is placed (white arrowhead) and motor layer where calcium responses are recorded. The red color indicates regions with significant elevation in the Ca^{++} signal. In the intact condition, stimulation of the sensory layer evokes a Ca^{++} response in the motoneurons (**D2**). After the fiber layer is cut (dotted line in**E1**), the motor layer responses were eliminated (**E2**). In this case, Ca^{++} responses around the stimulating electrode remained, indicating that the electrical stimulation of the sensory layer was still effective.

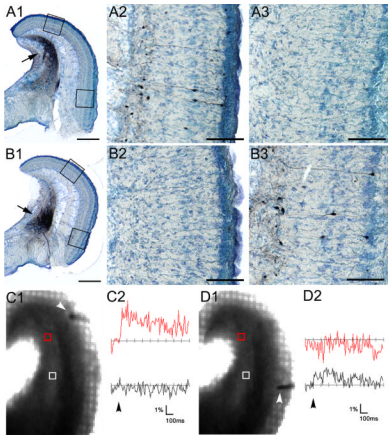

Figure 6.

Topographic organization of the goldfish vagal reflex system. **A, B:** Micrographs showing the results of small biocytin injections into the motor layer. Restricted injection into dorsal motor layer (arrow, **A1**) labeled VRIs only in the dorsal sensory layer (**A2**), not in the ventral one (**A3**). In the case of ventral injection (arrow, **B1**), labeled VRIs were distributed in the ventral sensory layer (**B3**), not in the dorsal (**B2**). These in vitro findings confirm our previous in vivo tracer study (Goehler & Finger, 1992). **C, D:** Micrographs (left) and graphs (right) showing calcium imaging experiment with topographic stimulation. Micrographs were captured under visible light after the recording to indicate the site of the stimulating electrode. Each black and red trace represents the signals obtained from the regions indicated as white and red squares, respectively, in the micrographs. When the stimulating electrode was placed in the dorsal sensory layer (white arrowhead, **C1**), calcium responses were elicited following the electrical stimulation in the dorsal motor layer, not in the ventral one (**C2**). Ventral sensory layer stimulation induced calcium responses in the ventral but not dorsal motor layer (**D2**). The same vagal lobe slice was used in C and D. Bar scale = 500 μm (A1, B1), 100 μm (A2, 3, B2, 3).

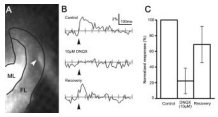

Figure 7.

Effects of the antagonist for AMPA/kainate receptors, DNQX, on the responses of vagal motoneurons. **A:** Micrograph of living vagal lobe slice for the pharmacological experiment captured by CCD camera. In pharmacological experiments, the sensory layer was cut off and the stimulating electrode (white arrowhead) was placed in fiber layer (FL) to directly stimulate axons of VRIs. **B:** Graph showing one example of the evoked vagal motoneuron calcium responses by electrical stimulation from single slice under control conditions with aCSF (upper), in the presence of 10 μM DNQX for 9 minutes (middle), and during recovery from DNQX following 45 minutes in normal aCSF (lower). Note that evoked calcium responses were suppressed by application of 10 μM DNQX. **C:** Histogram showing average of the vagal motoneuron calcium responses after DNQX application and washout. Responses were normalized to control response prior to DNQX application. n = 17 cells from 3 slices.

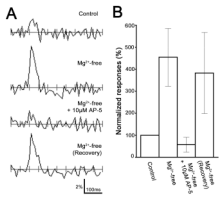

Figure 8.

Effects of Mg^{2+}-free conditions and application of 10 μM AP-5, competitive NMDA receptor antagonist for the vagal motoneurons activity. **A:** Traces illustrating the evoked calcium responses of the vagal motoneurons by electrical stimulation under control conditions in standard aCSF (upper) ; in Mg^{2+}-free aCSF (second) -- note that the enhance of the responses; in the presence of 10 μM AP-5 dissolved in Mg^{2+}-free aCSF for 9 minutes (third) -- note the elimination of enhanced response; and during washout of AP-5 following 30 minutes in Mg^{2+}-free aCSF (lower). **B:** Histogram showing average of the vagal motoneuron calcium responses after the incubation into Mg^{2+}-free aCSF, AP-5 application, and washout. Responses were normalized to control response prior to Mg^{2+}-free aCSF incubation. n = 13 cells from 3 slices.

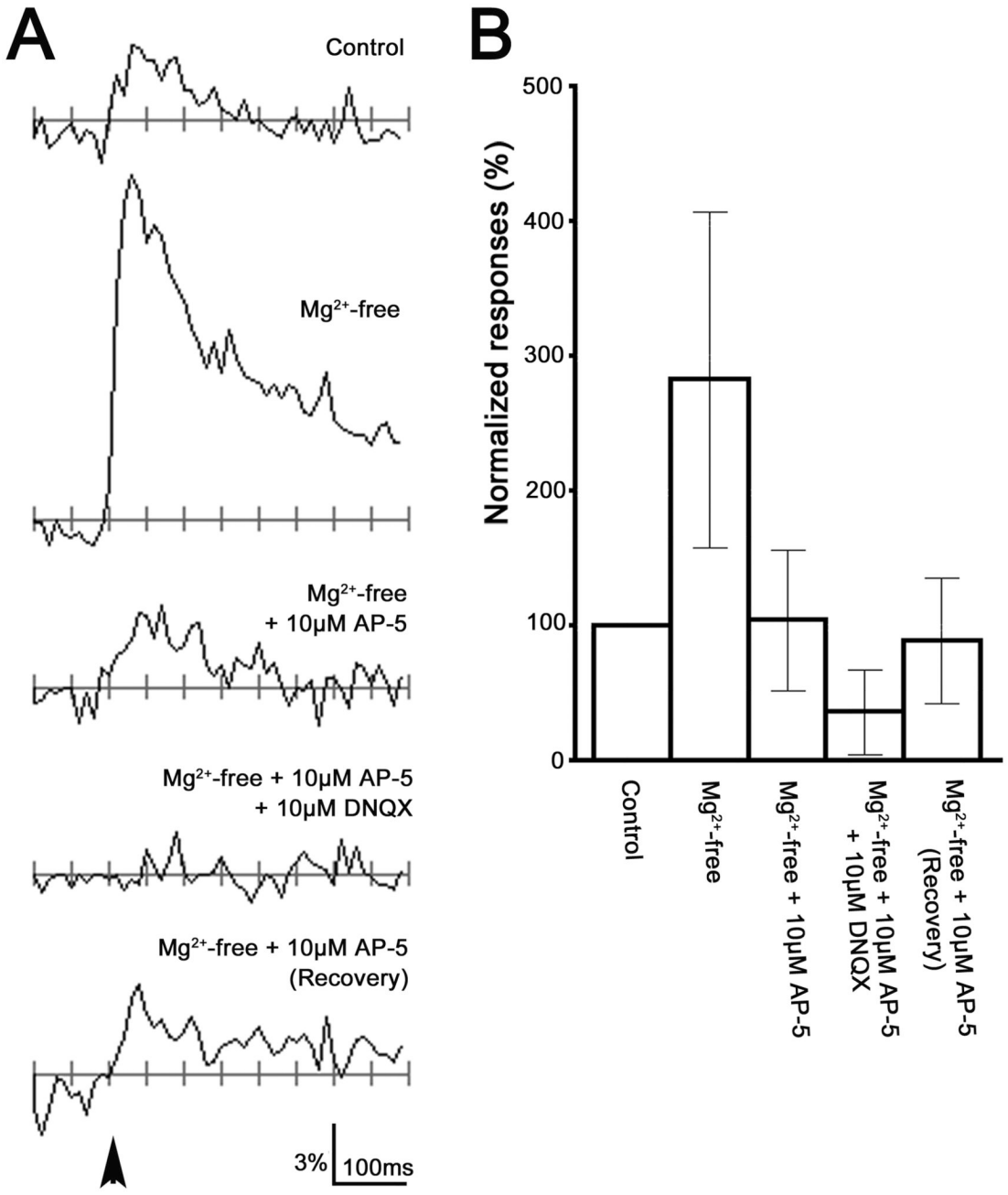

Figure 9.

A: As in Fig 8A, the first three traces show calcium responses of the vagal motoneurons under various conditions. Application of 10μM AP-5 eliminated the enhanced calcium responses but small responses remained (center panel). The remaining responses were removed by the further addition of 10μM DNQX (9minutes). **B:** Histogram showing average of the vagal motoneuron calcium responses after the incubation into Mg^{2+}-free aCSF, AP-5 and DNQX application, and washout. Responses were normalized to the control response prior to Mg^{2+}-free aCSF incubation. n = 14 cells from 3 slices.

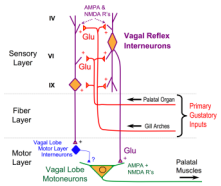

Fig. 10.

Schematic diagram showing the essential circuitry of the vagal reflex system involved in intraoral food-sorting. Primary Gustatory Inputs from the palatal organ (roof of the mouth) and gill arches (floor of the mouth) terminate within different sublaminae of the sensory layer of the vagal lobe. The primary afferents synapse with dendrites of interneurons (not shown) and Vagal Reflex Interneurons which send axons across the fiber layer to terminate on both interneurons and Vagal Lobe Motoneurons. Both the primary afferents and the Vagal Reflex Interneurons release glutamate which acts on post-synaptic AMPA/kainate (AMPA+) and NMDA receptors (R's) on the postsynaptic cells.